Oxidative dehydrogenation of propane on V_2O_5/ZrO_2 catalyst

Mahuya De and Deepak Kunzru*

Department of Chemical Engineering, Indian Institute of Technology, Kanpur, Kanpur 208016, India

Received 12 January 2004; accepted 14 April 2004

The performance of zirconia supported vanadia catalyst has been investigated for the oxidative dehydrogenation of propane. Vanadia loading was varied from 1.6 to 22.7 wt%, both below and well above monolayer coverage. The turnover frequency was highest for the catalyst with a vanadia surface density of 5 VO_x/nm^2. The effect of vanadia loading on the redox behavior of the catalysts was investigated by temperature-programmed reduction and temperature-programmed oxidation. The specific activity increased with ease of reducibility of the catalyst. The extent of reduction and ease of reoxidizability of the catalysts were also found to depend on the surface vanadia structure and to influence the catalytic activity. The effect of vanadia loading on the basicity of the catalysts was also investigated.

KEY WORDS: vanadia–zirconia; oxidative dehydrogenation; propane; temperature-programmed reduction; temperature-programmed desorption; redox properties.

1. Introduction

Oxidative dehydrogenation (ODH) of hydrocarbons has been extensively studied over supported vanadia catalysts. Support plays an important role in heterogeneous catalytic reactions. It promotes the reactions not only by enhancing the surface area and thereby increasing the metal dispersion but also by interacting with the active metal. The most commonly used supports are silica, alumina and titania. Recently zirconia, usually used as a ceramic material, is also attracting attention. It can be used either as a support [1–3] or as an active material [4–5]. The important properties that favor zirconia over the conventional supports include strong interaction with the active metal phase resulting in higher dispersion as well as higher thermal and chemical stability. It is reported to be stable even under reducing conditions [6]. Zirconia is the only metal oxide possessing all the four chemical properties important for catalysis: acidity, basicity, reducing ability and oxidizing ability. These unique features of zirconia make it suitable as catalytic material for many reactions. Currently, it is widely used either as a single support or mixed support for vanadia catalysts in various reactions. The major reactions that have been studied using vanadia–zirconia catalyst include decomposition of 2-propanol [7], complete oxidation of benzene [8], combined removal of NO_x and chlorinated hydrocarbons [9], partial oxidation of ethanol [10], ammoxidation and oxidation of toluene [11], alkylation of phenol [12], oxidation of sulfur dioxide [13] as well as ODH of hydrocarbons [14–16].

The activity and selectivity of supported vanadia catalysts are strongly affected by the oxidation state and molecular structure of surface vanadia species, which in turn depend upon the extent of metal-support interaction. Besides the nature of support, the preparation methods, pretreatment conditions and as well as the amount of vanadia content strongly influences the interaction of vanadia with the support.

Khodakov *et al.* [15] reported the performance of zirconia supported vanadia catalyst for ODH of propane at low conversions (below 1%), and correlated it with vanadia surface density. They concluded that polyvanadate species are more active than either monovanadate or crystalline species. Albrecht *et al.* [14] also studied the alkali modified and unmodified vanadia–zirconia catalyst for ODH of propane. They proposed that both monovanadates and polyvanadate species are active. Gao *et al.* [16] also concluded that both the species are active for ODH. However, there is still some controversy regarding the most selective site for ODH of propane.

It is well accepted that the ODH reactions on supported vanadia catalyst proceed *via* the Mars–van Krevelen mechanism consisting of reduction of the oxide catalyst surface by hydrocarbon and subsequent reoxidation by gas phase oxygen [17–19]. The redox property of the catalyst is therefore expected to play an important role in these reactions. Reducibility of vanadia supported on TiO_2, Al_2O_3 or SiO_2 has been shown to correlate with the activity trend of these catalysts in partial oxidation of methanol, ethane, toluene, *o*-xylene and ODH of propane [20–24]. It is generally observed that higher the reduction temperature (i.e. lower the reducibility), lower is the activity of the catalyst. On the other hand, the acid–base property of the catalyst can influence the adsorption–desorption of the reaction intermediates and products on the catalyst surface and thereby affect the process selectivity [25].

*To whom correspondence should be addressed.
E-mail: dkumzru@iitk.ac.in

1011-372X/04/0700–0033/0

The present study investigates the effect of reducibility and reoxidizability of the zirconia supported vanadia for ODH of propane. The vanadia loading was varied to investigate the effect of different surface vanadia species on the redox property and thereby on the performance of the catalyst. For this purpose, the catalysts were subjected to several cycles of reduction and oxidation. Such studies have not been reported earlier for vanadia–zirconia system. The redox property of the catalyst was characterized by temperature-programmed reduction (TPR) and temperature-programmed oxidation (TPO) whereas temperature-programmed desorption (TPD) of CO_2 and TPD of O_2 were used to determine the basicity and stability of the supported vanadia, respectively. To further elucidate the surface vanadia structure, the catalysts were characterized by Raman spectroscopy, X-ray diffraction and surface area measurements.

2. Experimental

2.1. Preparation

Zirconia support was prepared by dropwise addition of zirconyl nitrate solution to ammoniacal hydroxide solution. The pH was maintained between 11 and 12. The slurry of precipitated zirconium hydroxide was then aged under reflux for 12 h at 100 °C. It was cooled to room temperature and kept overnight. The precipitate was filtered, dried at 120 °C for 24 h and then calcined at 500 °C for 5 h.

Vanadia–zirconia catalysts were prepared by wet impregnation. The impregnating solution contained required amount of ammonium metavanadate and oxalic acid in 1 : 2 molar ratio. After impregnation, the thick slurry was dried at 120 °C in air with occasional stirring to yield a solid cake. After overnight drying at the same temperature, the catalyst was crushed and finally calcined at 500 °C for 5 h. The vanadia loading was varied from 1.6 to 22.7 wt%. The corresponding variation in vanadia surface density, defined as the number of vanadium atoms per square nanometer of surface area, was from 1 to 18 VO_x/nm_2. The catalysts have been designated as xVZrO, where x represents the vanadia surface density. Bulk V_2O_5 was prepared by decomposing ammonium metavanadate at 500 °C for 5 h.

2.2. Catalyst characterization

The surface area of a catalyst sample was measured by nitrogen physisorption using the dynamic pulsing technique on a Micromeritics Pulse Chemisorb 2705 unit. Before area measurements, all the samples were pretreated in a flow of helium (20 cc/min) at 25 °C for 45 min. Nitrogen was used as the adsorbent. The total gas flow rate (30% N_2 in He) was maintained at 16 cc/min.

X-ray diffraction spectra were obtained on a Reich Seifert (Germany) Iso Debye Flex X-ray diffractometer using Ni filtered monochromatic CuK_α radiation of wavelength 1.5418 Å. Scans were made in the 2θ range of 15°–80° at a scanning rate of 3°/min.

Ambient Raman spectra were recorded using a Bruker Equinox 55 FT-IR equipped with Raman accessory. The resolution of the spectrometer was 4 cm^{-1}. Nd:YAG laser was used as the laser source and operated at a power level of 200 mW. Powdered sample mixed with KBr (1 : 30) was placed in the quartz tube and 90° excitation geometry was used for analysis.

TPR, TPO and TPD studies were performed on the Micromeritics Pulse Chemisorb 2705. For each test, 50 mg of sample was pretreated in an oxidative atmosphere (5% O_2 in He) at 500 °C for 30 min and cooled to 250 °C in the same mixture. The sample was then purged with helium and cooled to room temperature. For TPR studies, preoxidized samples were reduced in a flow of 5% H_2 in argon from room temperature to 950 °C. For TPO, 5% O_2 in He was used as the carrier gas. Each TPR cycle was followed by a TPO cycle. For TPD of O_2 , the samples were heated to 800 °C in flowing helium. For the TPD of CO_2, the preoxidized samples were saturated with pulses of CO_2 (0.1 mL) followed by flushing in helium for 30 min. The TPD was carried out in flowing helium. For each test, the carrier gas flow was maintained at 30 mL/min with a heating rate of 10 K/min.

2.3. Catalyst activity measurements

The activity of the catalysts for ODH of propane was measured in the temperature range of 300–450 °C at atmospheric pressure using a tubular downflow quartz reactor. The feed mixture contained propane, oxygen and nitrogen in the molar ratio of 4/4/92. The mass of the catalyst was varied from 100 to 250 mg and the total flow rate from 50 to 150 cc/min. Prior to testing, the catalyst was treated in a flow of oxygen at 500 °C for 30 min. The average run length was 30 min. The reaction products were analyzed online by two gas chromatographs. For all the runs reported, the carbon balance was 100 ± 5%. At the highest reaction temperature used in this study, the catalyst showed no significant deactivation even after a run length of 650 min. Catalytic activities have been expressed in terms of conversion of propane (%) and selectivity (%), defined as:

$$\text{Conversion}(\%) = \frac{\text{moles of carbon in products}}{\text{total moles of carbon in exit gas}} \times 100$$

$$\text{Selectivity of product 'X'}(\%) = \frac{\text{moles of carbon in product 'X'}}{\text{total moles of carbon in products}} \times 100$$

Table 1
Variation of surface area with vanadia loading

Catalyst	Vanadia loading (wt%)	Surface area (m^2/g)	Surface density[a] (VO_x/nm^2)
ZrO2	0	107.9	0
1VZrO	1.6	107.9	1.0
2VZrO	3.1	104.8	2.0
5VZrO	7.4	99.9	4.9
8VZrO	11.3	86.7	7.8
12VZrO	16.1	70.6	11.7

[a]Based on the surface area of support.

3. Results and discussion

3.1. Catalyst characterization

3.1.1. Surface area and XRD

Table 1 shows the surface area of the catalysts with different vanadia surface density. The surface area decreased with an increase in vanadia surface density. Other investigators have also reported such a trend [26–28]. The decrease in surface area may be the result of plugging of pores by impregnated vanadia.

The X-ray diffraction spectra of vanadia–zirconia catalysts are shown in figure 1. For pure zirconia, the tetragonal phase is characterized by a peak at $2\theta = 30.4°$ and monoclinic phase by peaks at $2\theta = 28.5°$ and $31.6°$ [29–30]. The zirconia used in our study mainly consisted of tetragonal phase as shown by figure 1. The tetragonal phase was stable and was not significantly affected by vanadia impregnation. The XRD patterns of the catalysts did not show any characteristic peaks of crystalline V_2O_5 ($2\theta = 20.3°$ and $26.2°$) up to vanadia density of 12 VO_x/nm^2. Presence of these peaks was observed for 18VZrO catalyst. However there was no indication of formation of a mixed phase containing vanadia and zirconia in any catalyst.

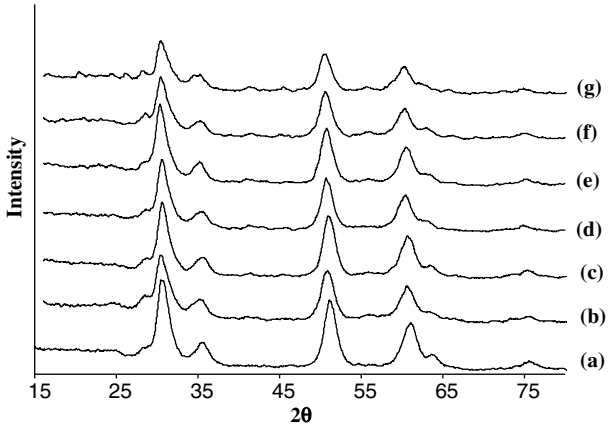

Figure 1. XRD pattern of the vanadia–zirconia catalysts: (a) ZrO_2; (b) 1VZrO; (c) 2VZrO; (d) 5VZrO; (e) 8VZrO; (f) 12VZrO; (g) 18VZrO.

3.1.2. Raman spectroscopy

Ambient Raman spectra of the catalysts are shown in figure 2. The peaks at 268, 316, 382, 474, 615 and 640 cm^{-1} can be ascribed to ZrO_2 phase and are increasingly masked by the colored vanadium oxide overlayer as vanadia loading increases. The broad band from 700–970 cm^{-1} in the catalysts with vanadia coverage of 5 VO_x/nm^2 and above is characteristic of V–O–V stretching mode of polyvanadate species [15,31]. The intensity of the polyvanadate band increased with increasing vanadium loading. The shifting of the band to higher wave number with increasing vanadia loading is attributed to the increase in average chain length with loading. It is generally accepted that at very low vanadia surface density (< 2 VO_x/nm^2), tetrahedral monovanadate species are predominant and further increase in vanadia density leads to formation of polyvanadate species [32]. The peak at 1028 cm^{-1} corresponds to the stretching of the terminal V=O bond in isolated vanadyl species. The low vanadia loaded catalysts do not show any sharp peak at this wave number most probably due to the hydrated state of these species under ambient condition [33]. Instead a weak broad band between 900 and 1000 cm^{-1} is observed for hydrated vanadyl groups as also reported by Cristiani *et al.* [34]. Laser induced dehydration may be the cause of appearance of the terminal V=O peak in the higher vanadia loaded catalyst. The crystalline V_2O_5, characterized by the peaks at 283, 305, 405, 485, 527, 702 and 996 cm^{-1}, first appears in the higher loaded catalyst, 8VZrO, indicating the formation of monolayer coverage. The most intense

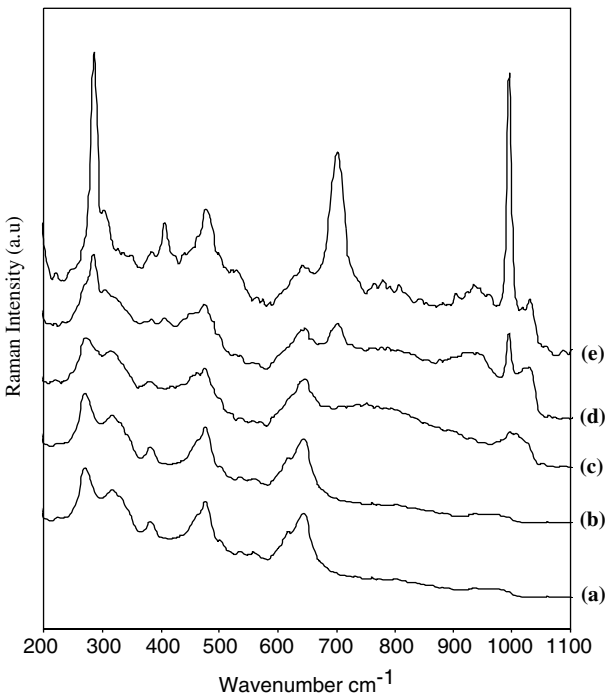

Figure 2. Ambient Raman spectra of vanadia–zirconia catalyst: (a) 1VZrO; (b) 2VZrO; (c) 5VZrO; (d) 8VZrO; (e) 12VZrO.

of these bands at 996 cm^{-1} is primarily due to the symmetric stretching of V=O group in the bulk.

3.1.3. Temperature programmed desorption of O_2

The desorption profiles of oxygen from freshly oxidized zirconia supported vanadia catalysts are shown in figure 3. For comparison, desorption profiles for the bulk vanadia and zirconia have also been shown. For bulk vanadia, there were two distinct peaks at 640 and 650 °C, whereas for zirconia, no peaks were obtained in this temperature range. For supported vanadia catalysts a single broad peak was observed, and the peak maxima shifted to lower temperatures with an increase in vanadia loading. However, at lower loadings (< 5 VO_x/nm^2) no peak was detected. These TPD profiles suggest that the structure of vanadia is modified when supported on zirconia and the interaction results in oxygen bond energies different than that in bulk vanadia. The appearance of a single oxygen peak implies that only one kind of oxygen is desorbed whereas in case of bulk vanadia at least kinetically two different types of oxygen exist. The amount of desorbed oxygen (table 2) shows that for the catalysts having surface vanadia density higher than monolayer coverage (≥8 VO_x/nm^2), a constant amount of oxygen was desorbed, independent of loading. The total amount of oxygen desorbed constituted only a very small fraction of the total oxygen present in the lattice, therefore no major change in the structure is expected. The fraction of oxygen desorbed in case of supported vanadia was an order magnitude higher than that of bulk vanadia, which indicates that the modified structure of the supported catalysts results in higher concentration of labile oxygen.

Table 2
Amount of oxygen desorbed from bulk and supported vanadia

Catalyst	O_2 desorbed atoms/gm	Desorbed O_2 / Total O_2
1VZrO	nd[a]	nd
2VZrO	nd	nd
5VZrO	4.5×10^{19}	0.037
8VZrO	6.1×10^{19}	0.032
12VZrO	6.1×10^{19}	0.023
18VZrO	6.2×10^{19}	0.016
V_2O_5	2.4×10^{19}	0.001

[a] nd, Not detected.

3.1.4. Temperature-programmed reduction/temperature-programmed oxidation

The successive TPR and TPO profiles of bulk V_2O_5 are plotted in figures 4 and 5, respectively. Each

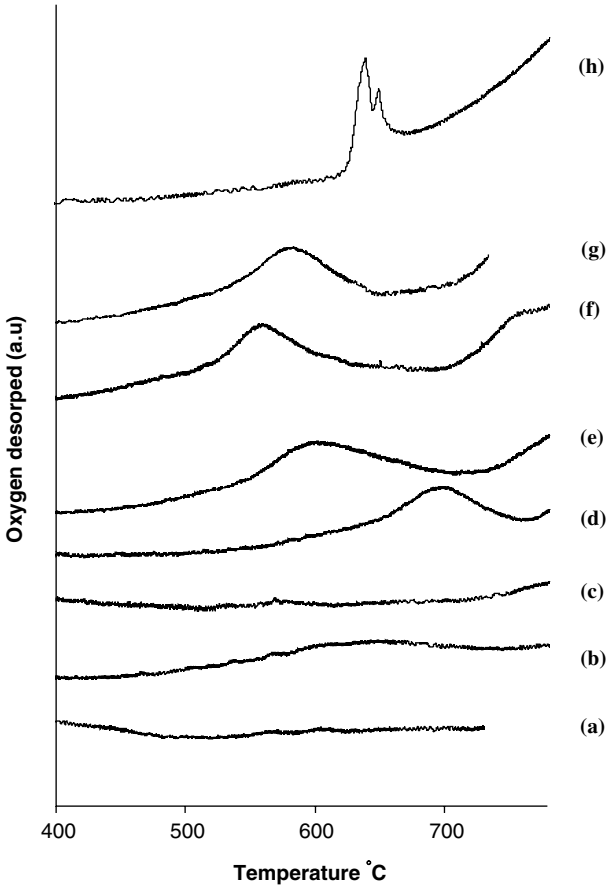

Figure 3. Temperature-programmed desorption of oxygen for: (a) ZrO_2; (b) 1VZrO; (c) 2VzrO; (d) 5VzrO; (e) 8VzrO; (f) 12VzrO; (g) 18VzrO; (h) V_2O_5.

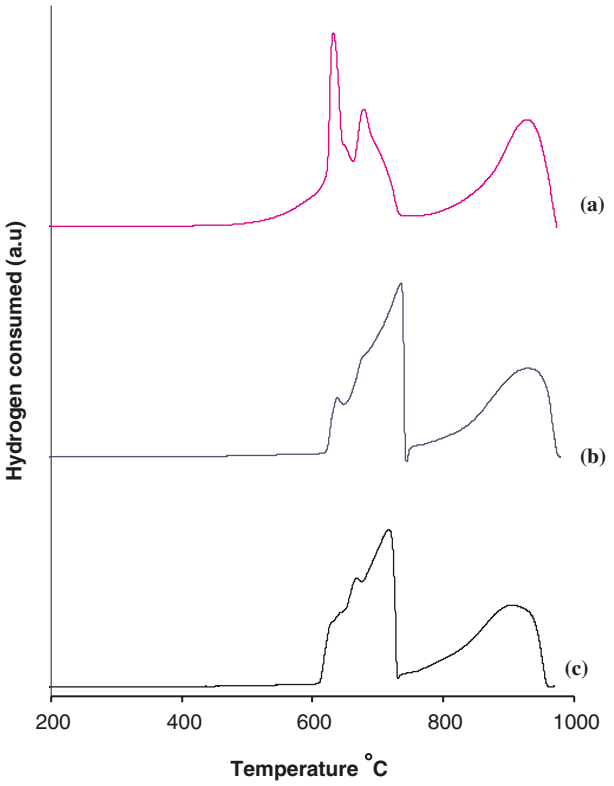

Figure 4. TPR profiles of bulk vanadia: (a) 1st TPR cycle; (b) 2nd TPR cycle (c) 3rd TPR cycle.

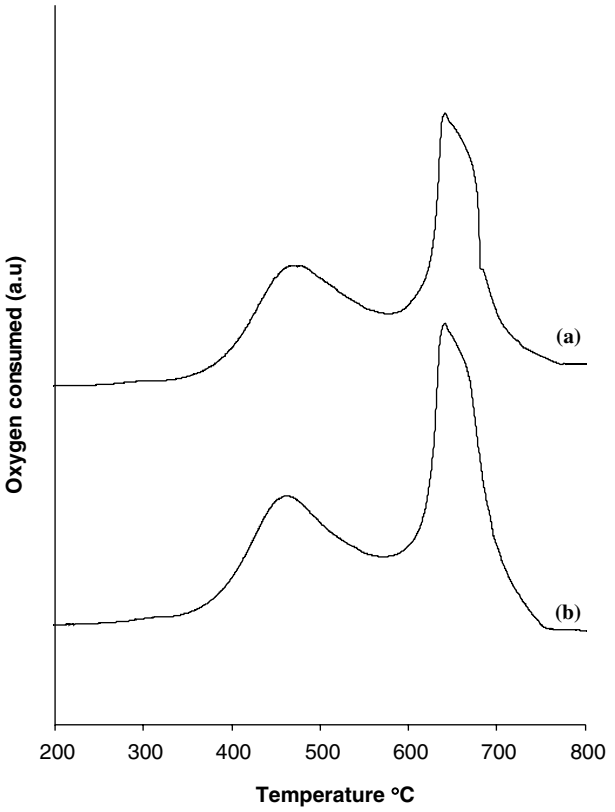

Figure 5. TPO profiles of bulk vanadia: (a) 1st TPO cycle; (b) 2nd TPO cycle.

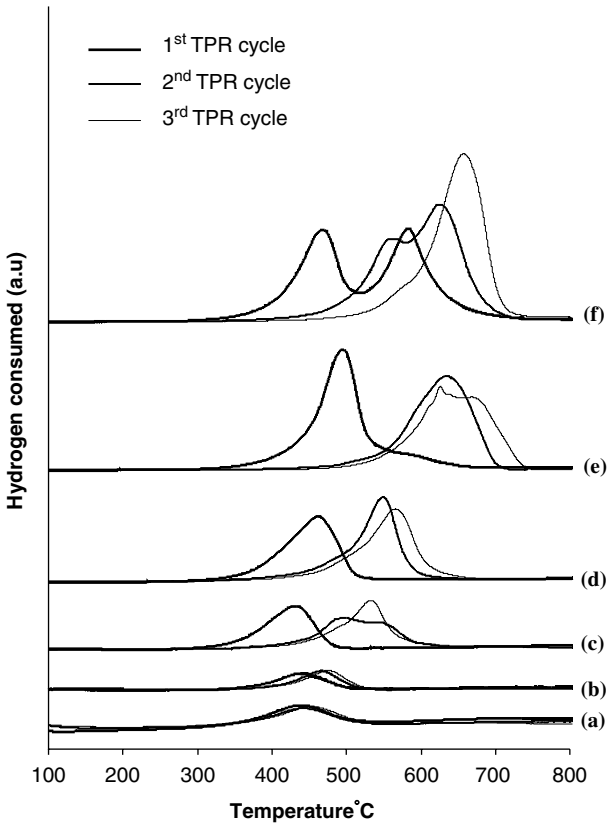

Figure 6. TPR profiles of vanadia–zirconia catalysts: (a) 1VzrO; (b) 2VzrO; (c) 5VzrO; (d) 8VzrO; (e) 12VzrO; (f) 18VzrO.

reduction run was followed by TPO. As can be seen in figure. 4a, the first reduction profile of V_2O_5 has three major peaks at 632, 680 and 852 °C. Presence of multiple peaks suggests reduction of vanadia *via* several steps. It has been proposed that vanadia reduction occurs in four steps [35]:

$$V_2O_5 \rightarrow V_6O_{13} \rightarrow V_2O_4 \rightarrow V_nO_{2n-1} \rightarrow V_2O_3$$

The asymmetric nature of the second peak in the figure 4a shows the presence of a shoulder around 715 °C which may correspond to the reduction to magneli phases of vanadia. Successive redox cycles resulted in a significant decrease in the intensity of the first peak at 632 °C with a simultaneous increase in the intensity of the second peak. The intensity of the shoulder at 715 °C markedly increased. However, repetitive reduction cycles did not have a significant effect either on the position of the peaks or on the intensity of the last peak. The TPO profiles shown in figure 5 are characterized by two major peaks at 470 and 630 °C. Successive cycles did not have any significant effect on the peak position or intensity. The second peak was quite asymmetric in nature, as also reported by Kim and Lee [36], and very likely consists of two oxidation peaks.

The successive TPR profiles of the vanadia dispersed on zirconia are shown in figure 6. The first reduction cycles of the catalysts up to vanadia loading of 12 VO_x/nm^2 show that, in contrast to bulk vanadia, these catalysts reduced only in one step and at a much lower temperature, signifying strong metal-support interaction. The catalyst with high vanadia loading (18 VO_x/nm^2) showed multiple peaks. The catalyst with a surface density of 5 VO_x/nm^2 showed the lowest reduction temperature (T_{max}). For a surface density of 1 VO_x/nm^2, the reduction temperature was higher than that for a loading of 2 VO_x/nm^2. This was confirmed by repeated experiments. Beyond a surface density of 5 VO_x/nm^2, T_{max} shifted to higher values. As can be observed from figure 6, beyond monolayer coverage there was an increase in the reduction temperature. The increase in T_{max} probably occurs due to an increase in both the diffusion limitation as well as oxygen bond energy. For all catalysts, in successive TPR cycles, the peak maxima shifted to higher temperatures. For catalysts having surface density $\geq$ 5 VO_x/nm^2, multiple peaks appeared. The appearance of the multiple peaks suggests that successive reduction–oxidation cycles results in aggregation of some of the surface vanadia species.

The H/V ratio for all the catalysts is given in table 3. For bulk vanadia, H/V ratio was found to be 2 corresponding to stoichiometric reduction from V^{5+} to V^{3+}. With increasing vanadia loading, extent of reduction increased as shown by the increasing H/V ratio. For 18VZrO it was same as that for bulk vanadia. For low vanadia loaded catalysts, the extent of reduction

Table 3
H/V ratio for the bulk and supported vanadia for all the TPR cycles

Catalyst	TPR 1	TPR 2	TPR 3
1VZrO	1.2	1.1	1.1
2VZrO	1.4	1.4	1.4
5VZrO	1.6	1.7	1.7
8VZrO	1.6	1.8	1.8
12VZrO	1.7	1.8	1.8
18VZrO	2	2	2
V_2O_5	2	2	2

decreased or remained the same for subsequent reduction cycles but that for high vanadia loading increased. Zirconia was also reduced under identical conditions but no peaks were obtained up to 950 °C.

The TPO profiles of the reduced supported vanadia are shown in figure 7. As for the case of bulk vanadia, oxidation occurred at a lower temperature than the reduction. Only one peak was observed at lower vanadia coverage ($\leq$8 VO_x/nm^2) while two peaks were obtained for catalysts with higher vanadia surface density.

3.1.5. *Temperature programmed desorption of CO_2*

The vanadium atoms having nonbonding d orbitals with lowest unoccupied molecular orbital (LUMO) character show Lewis acidity and bridging oxygen with lone-electron pair act as a Lewis base. The coordinately unsaturated vanadium and oxygen ions develop Bronsted acid–base interaction. Acidic CO_2 can adsorb on all these basic sites. The total basicity, expressed in terms of μmol of CO_2 adsorbed per gm of sample, is shown in table 4. The amount of CO_2 adsorbed on zirconia is in good agreement with the results of Nagai *et al.* [37], who reported a value of 116 μmol CO_2/g cat. The higher value measured for our support may be due to the higher surface area. The desorption temperature is related to the strength of basic site; higher the desorption temperature, higher is the site strength. The TPD profile (figure 8a) of pure zirconia shows presence of weak basic sites corresponding to the low temperature peak around 90–100 °C whereas the higher temperature peak is due to the basic sites of medium strength [38–40].

Table 4
Variation in basicity with vanadia loading for vanadia–zirconia catalysts

Sample	Basicity (μmol CO_2/g of catalyst)
ZrO_2	136
1VZrO	64
2VZrO	23
5VZrO	15
8VZrO	0.38
12VZrO	0.12

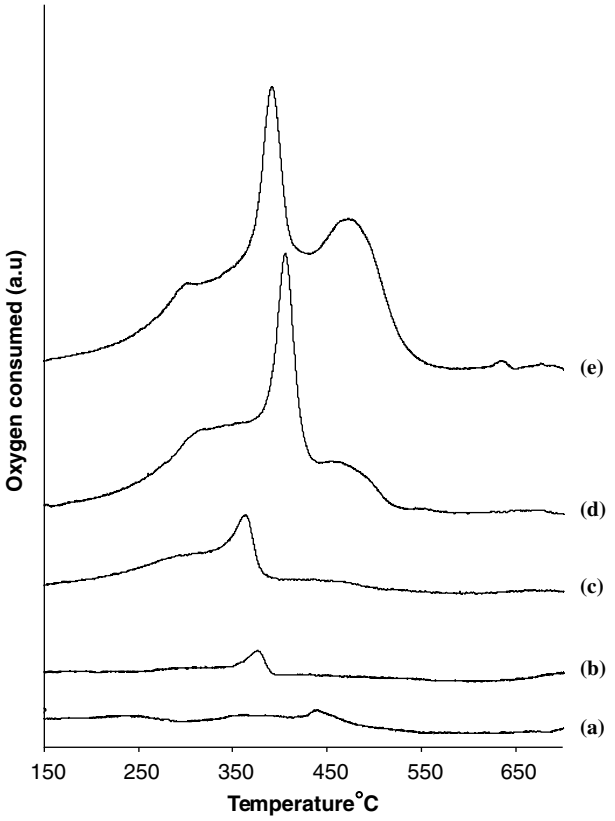

Figure 7. TPO profiles of vanadia–zirconia catalysts: 1VzrO; (b) 5VZrO; (c) 8VZrO; (d) 12VZrO; (e) 18VZrO.

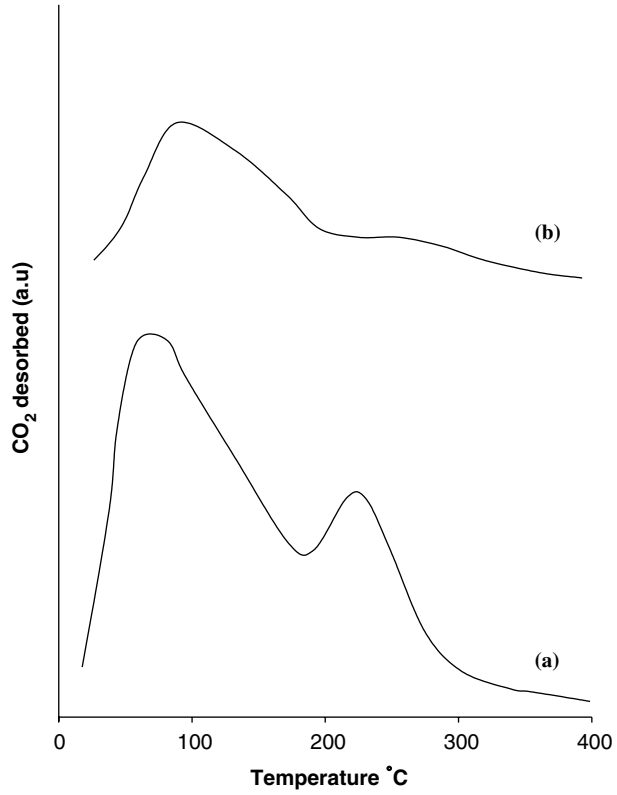

Figure 8. CO_2 -TPD profiles of (a) zirconia and (b) zirconia supported vanadia, 1VZrO.

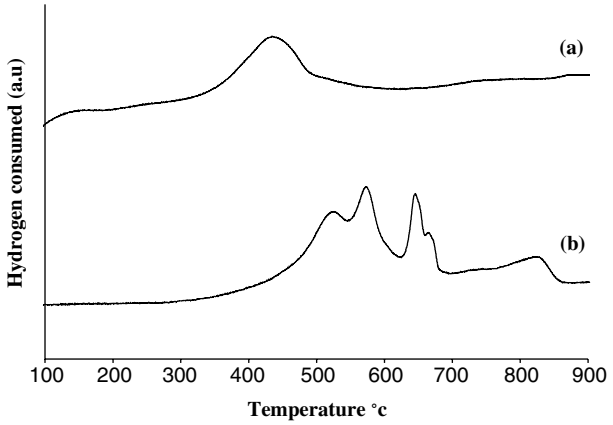

Figure 9. TPR profiles of used 5VZrO catalyst (a) 1st TPR cycle (b) 2nd TPR cycle.

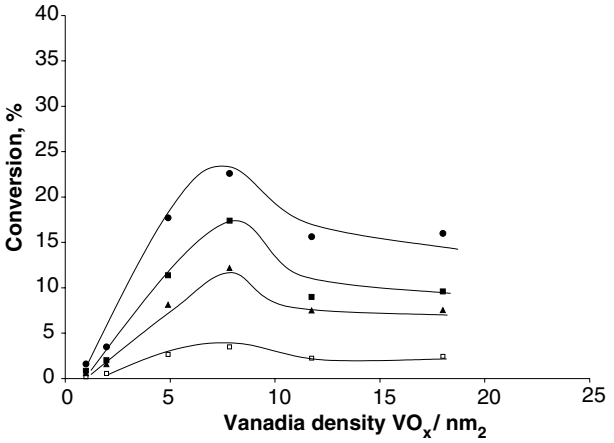

Figure 10. Variation of conversion with vanadia surface density at different temperatures ($W/F_{AO} = 5.4$ g cat. h/mol of propane). ●, 425 °C; ■, 400 °C; ▲, 385 °C; □, 335 °C.

It can be seen that deposition of 1.6% vanadia on zirconia (1VZrO) reduced the basicity of zirconia by nearly 50%. The remaining sites are mostly weak in nature as shown in figure 8b. With further increase in vanadia coverage, basicity decreased steadily.

3.1.6. *TPR of used catalyst*

To study the modifications in the catalyst properties during reaction, the TPR profiles of the used catalysts, without any oxidative pretreatment, were also obtained and a typical result for 5VZrO catalyst is shown in figure 9a. As compared to the fresh catalyst (figure 6), a broader peak was obtained in the first TPR cycle, with T_{max} being slightly lower. The second TPR cycle results in more number of peaks than that obtained for the fresh catalyst (figure 9b). The average oxidation state of the used catalyst, calculated from hydrogen consumption, was 4.42.

3.2. *Catalytic activity*

The activities of the catalysts, with vanadia surface density ranging from 1 to 18 VO_x/nm^2 were compared at identical conditions. The variation of conversion with vanadia surface density at different temperatures is shown in figure 10. At all temperatures, the conversion of propane passed through maxima at a vanadia surface density of approximately 8 VO_x/nm^2. Similar variations of conversion with vanadia surface density were also observed at other contact time of 21.4 and 5.3 g cat. h/mol of propane. The turnover frequencies (TOF s^{-1}, i.e. molecules of propane consumed per second per vanadium atom) at 335 °C are shown in table 5. The TOF values were highest for 5 VO_x/nm^2. Turnover frequency for V_2O_5/ZrO_2 at identical conditions is not available in the published literature. For a C_3H_8/O_2 ratio of 8 : 1 and at low conversion (< 1%) Khodakov *et al.* [15] have reported TOF values between 1 and 3.5×10^{-3} s^{-1} at 333 °C for V_2O_5/ZrO_2 catalysts calcined at 773 K.

Table 5
Turn over frequency (TOF) of vanadia–zirconia catalysts at 335 °C

Catalyst	TOF $s^{-1} \times 10^{-3}$
1VZrO	0.6
2VZrO	0.7
5VZrO	1.7
8VZrO	1.5
12VZrO	0.7
18VZrO	0.5

The main reaction products were propene, carbon monoxide and carbon dioxide. At higher temperatures, small amount of ethylene (< 0.5%) was also obtained. To determine the primary and secondary products, for each catalyst, runs were taken at isothermal conditions for different W/F_{AO}, where W is the weight of catalyst in grams and F_{AO} is the molar flow rate of propane, and the results for 12VZrO catalyst at 335 °C are shown in figure 11. As can be seen from this figure, during ODH of propane, C_3H_6, CO and CO_2 are formed as primary products. Moreover, the secondary reactions of propene mainly result in formation of CO as selectivity of CO_2 remains almost constant. The variation of initial product selectivities with vanadia surface density at 330 °C is shown in figure 12. The initial selectivities of propylene increased with vanadia loading upto a vanadia surface density of 8 VO_x/nm^2,and thereafter leveled off at higher vanadia loadings. This trend is in agreement with the results reported by Khodakov *et al.* [15]. However, maximum selectivity reported in our case is lower which may be due to the different method of catalyst preparation and reaction conditions used.

For comparison, the activities of bulk vanadia and zirconia were also determined. Both pure zirconia and vanadia showed very low activity for propane ODH upto a temperature of 425 °C (table 6). Vanadia showed

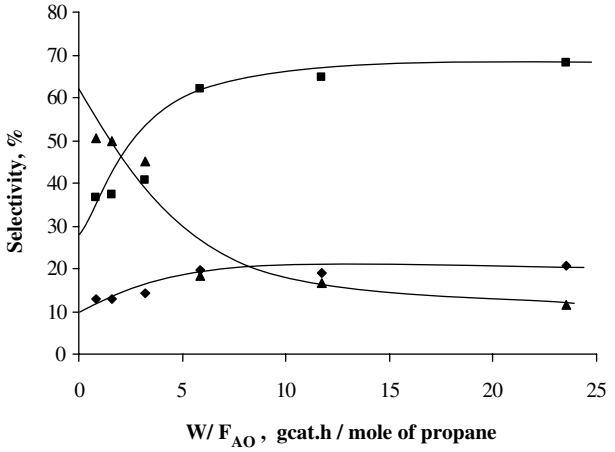

Figure 11. Selectivity of the products at 335 °C for 12 VZrO catalyst. ■, CO; ●, CO_2; ▲, propene.

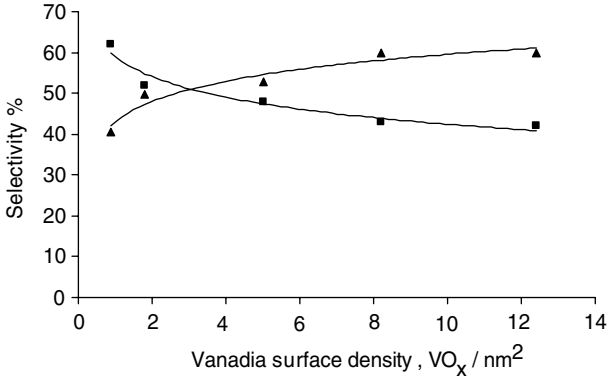

Figure 12. Variation of selectivity with vanadia surface density.

high selectivity for propene while zirconia favored combustion of propane.

3.3. Discussion

The surface area measurements, XRD analysis and Raman spectroscopy results agree well with the general model proposed for vanadia–zirconia catalyst by earlier studies [14–16]. The increase in vanadia loading resulted in a decrease in surface area probably due to pore blockage. The XRD results show that vanadia is well dispersed on the zirconia surface and for loading up to 12 VO_x/nm^2 , the metal aggregation, if any, was less than 4 nm since no additional peaks were detected. Centi [41] estimated the theoretical monolayer coverage for a monovanadate monolayer to be 2–3 and 7.5 VO_x/nm^2 for a polyvanadate monolayer. Wachs and Weckhuysen [42] determined the monolayer vanadia surface density on different supports from Raman spectroscopy measurements and found this to be in the range of 7–8 VO_x/nm^2, as also confirmed by our results.

The redox mechanism for ODH of propane can be summarized as:

Table 6
Activity of bulk vanadia and zirconia (W/F_{AO} = 5.4 g cat. h/mol of propane)

	Temperature (°C)	Conversion (%)	Selectivity of products		
			Propene	CO	CO_2
V_2O_5	425	0.8	60.2	21.8	18.0
	400	0.4	66.5	19.2	14.3
	385	0.3	65.8	19.7	14.6
ZrO_2	425	0.3	31.0	33.3	35.6
	400	0.2	43.8	27.0	29.2

$$\text{propane} + \text{lattice } O_2 \rightarrow \text{propene} + \square \quad (1)$$

$$2\square + \text{gaseous } O_2 \rightarrow \text{lattice } O_2 \quad (2)$$

where □ represents the oxygen vacancy in the lattice. Therefore, the reducibility and reoxidizability of the catalyst surface, which in turn depends on the oxygen bond energy of the catalyst, is an important factor in determining the activity of the catalyst. All the TPR profiles of first reduction cycle for vanadia surface density upto 12 VO_x/nm^2 showed only one peak at a much lower temperature than the bulk vanadia, confirming that surface vanadia species are more easily reducible than the bulk. The lowering of T_{max} in the range of 2–5 VO_x/nm^2 implies that polyvanadate species are more reducible than either monovanadates or bulk vanadia, which agrees with the results reported by Bañares *et al.* [21]. The greater reducibility of the polyvanadate species suggests lower oxygen bond energy for these species. If it is assumed that reduction of lattice oxygen by propane is the controlling step (equation 1) then the species with lower oxygen bond energy is expected to show higher activity. This is confirmed from the TOF frequency values (table 5) which shows that the catalyst with surface density 5 VO_x/nm^2 showed the highest activity. As shown by the characterization studies (figure 2), the concentration of polyvanadate species is higher for 8VZrO but due to the presence of small amount of crystalline vanadia, the TOF value is lowered. The lower activity of the crystalline vanadia may be due to both the higher oxygen bond energy and diffusion limitation. It should be mentioned that 8VZrO gave the highest conversion in spite of TOF value lower than 5VZrO. This can be explained on the basis of higher rate of reaction for 8VZrO where the rate of reaction, expressed as moles of propane reacted/(gm of catalyst)(s), is equal to the product of TOF and VO_x/g of catalyst. At still higher vanadia loading, the activity decreased due to an increase in crystalline vanadia. The lower activity of the monomeric species as compared to polyvanadates may be due to its higher oxygen bond energy (i.e. lower reducibility).

All the TPO profiles show that the reoxidation occurs at a much lower temperature as compared to reduction.

The easier reoxidizability of the catalysts makes the second step (equation 2) to be less likely as the rate controlling. This agrees with the model proposed by Chen *et al*. [19]. Further, the polyvanadate species are also found to be more easily reoxidized than either monovanadates or crystalline vanadia figure 7.

The H/V ratio for the stoichiometric reduction from $V^{5+} \rightarrow V^{4+}$ and $V^{5+} \rightarrow V^{3+}$ are 1 : 1 and 2 : 1, respectively. All the submonolayer and monolayer catalyst showed intermediate values of H/V ratio between these two extremes (table 3) which suggests that some fraction of vanadia either does not undergo any reduction or undergoes only partial reduction to V^{4+}. On the other hand, complete reduction occurs for higher vanadia loaded catalyst (18VZrO) and also for bulk vanadia. The difference in extent of reducibility is caused by the difference in the vanadia structures induced by the interaction with the support. The maximum activity of the polyvanadate species having intermediate values of H/V ratio suggests that optimum extent of reducibility of the catalyst is probably desirable for higher activity.

The first TPR profile of the used catalyst [figure 9a] shows its better reducibility compared to the fresh catalyst which has also been reported by Reiche *et al*. [43] for $V_2O_5^-$ WO_3/TiO_2 catalyst and was explained on the basis of restructuring phenomenon which may occur during reaction. The second TPR cycle of the used catalyst was different from that of the fresh one and resembled more the stepwise reduction pattern of crystalline vanadia (figure 8a). This supports the proposition that redox cycles during reactions modify the surface vanadia species which result in the difference in the TPR profiles. When the used catalyst was pretreated in pure oxygen before conducting the first TPR study, the resultant profiles were identical to that of the fresh catalyst. These results indicate that restructuring may have occurred during ODH of propane but reoxidation by pure oxygen results in retrieval of the original structure.

For supported catalyst, the lower selectivity at low vanadia loading may be due to exposed area of the support since at the same conversion, bulk zirconia shows lower selectivity to propene than that of bulk vanadia as discussed earlier. Selectivity increased with an increase in coverage and leveled off at coverages above monolayer. However, CO_2 desorption studies showed that the basicity of zirconia was considerably higher than supported vanadia catalyst. Thus it can be concluded that basicity is not the only property which determines the selectivity of these catalysts.

4. Conclusions

The results of the present study can be summarized as:

1. Redox behavior of the surface vanadia species is strongly influenced by its structure which in turn depends on the extent of loading.
2. Polyvanadate species are most easily reducible and reoxidizable than either monovanadates or bulk species.
3. Compared to monovanadates and bulk vanadia, polyvanadate species are more active for ODH of propane.
4. The combination of various factors such as oxygen bond energy, diffusion limitation, extent of reduction and concentration of labile oxygen results in higher activity of the polyvanadate species.
5. Reduction of the lattice oxygen is the rate determining step for the ODH of propane on zirconia supported vanadia catalysts.

Acknowledgments

We are very grateful to Indian Oil Corporation, R&D Centre, Faridabad for recording the Raman spectra.

References

[1] V. Indovina, Catal. Today 41 (1998) 95.
[2] V.V. Brei, S.V. Prudius and O.V. Melezhyk, Appl. Catal. A: Gen. 239 (2003) 11.
[3] D. Pietrogiacomi, M.C. Campa, S. Tuti and V. Indovina, Appl. Catal. B : Env. 41 (2003) 301.
[4] W.B. Johnson and J.G. Eckerdt, J. Catal. 126 (1990) 146.
[5] F.R. Chen, G. Coudurier, J.F. Jo and J.C. Vedrine, J. Catal. 143 (1993) 616.
[6] G.K. Chuah, S. Jaenieke, S.A. Cheong and K.S. Chan Appl. Catal. A: Gen. 145 (1996) 267.
[7] Y. Toda, T. Ohno, F. Hatayama and H. Miyata, Appl. Catal. A: Gen. 207 (2001) 273.
[8] D. Andreeva, T. Tabakova, L. Ilieva, A. Naydenov, D. Mehanjiev and M.V. Abrashe, Appl. Catal. A: Gen. 209 (2001) 291.
[9] J. Jones and J.R.H. Ross, Catal. Today 35 (1997) 97.
[10] J.M. Miller and L.J. Lakshmi, J. Catal. 184 (1999) 68.
[11] M. Sanati, A. Andersson, L.R. Wallenberg and B. Rebenstorf. Appl. Catal. A: Gen. 106 (1993) 51.
[12] K.V.R. Chary, K. Ramesh, G. Vidyasagar and V.V. Rao, J. Mol. Catal. A: Chem. 198 (2003) 195.
[13] J.P. Dunn, P.R. Koppula, H.G. Stenger and I.E. Wachs, Appl. Catal. B: Env. 19 (1998) 103.
[14] S. Albrecht, G. Wendt, G. Lippold, A. Adamski and K. Dyrek, Solid State Ionics 101–103 (1997) 909.
[15] A. Khodakov, J. Yang, S. Su, E. Iglesia and A.T. Bell, J. Catal. 177 (1998) 343.
[16] X. Gao, J. Jehng and I.E. Wachs, J. Catal. 209 (2002) 43.
[17] E.A. Mamedov and V. Cortés Corberán, Appl. Catal. A: Gen. 127 (1995) 1.
[18] D. Creaser, B. Andersson, R.R. Hudgins and P.L. Silveston, Appl. Catal. A: Gen. 187 (1999) 147.
[19] K. Chen, A. Khodakov, J.Yang, A.T. Bell and E. Iglesia. J.Catal. 186 (1999) 325.
[20] G. Deo and I.E. Wachs, J. Catal. 146 (1994) 323.
[21] M.A. Bañares, M.V. Martínez-Huerta, X. Gao, J.L.G. Fierro and I.E. Wachs, 61 (2000) 295.
[22] A.J. Van Hengstum, J.G. Van Ommen, H. Boseh and P.J. Gellings, Appl. Catal. A: Gen. 8 (1983) 369.
[23] S. Anniballi, F. Cavani, A. Guerrini, B. Panzacchi, F. Trifirò, C. Fumagalli, R. Leanza and G. Mazzoni, Catal. Today 78 (2003) 117.

[24] A.A. Lemonidou, L. Nalbandian and I.A. Vasalos, 61 (2000) 333.
[25] T. Blasco and J.M. Lopez Nieto, Appl. Catal. A: Gen. 157 (1997) 117.
[26] E.V. Kondratenko and M. Baerns, Appl. Catal. A: Gen. 222 (2001) 133.
[27] N.V. Economidis, D.A. Peña and P.G. Smirniotis Appl. Catal. B: Env. 23 (1999) 123.
[28] A.R.J.M. Mattos, R. Aguiar da Silva San Gil, Maria Luiza M. Rocco and J.G. Eon, J. Mol. Catal. A: Chem 178 (2002) 229.
[29] H. Toraya, M. Yoshimura and S. Somiya, J. Am. Ceram. Soc. 67 (1984) C-119.
[30] G.K. Chuah and S. Jaenicke Appl. Catal. A: Gen. 163 (1997) 261.
[31] G.T. Went, S.T. Oyama and A.T. Bell, J. Phys. Chem. 94 (1990) 4240.
[32] B. Grybowska, Appl. Catal. A: Gen. 157 (1997) 409.
[33] G. Deo and I.E. Wachs, J. Phys. Chem. 94 (1990) 4240.
[34] C. Cristiani, P. Forzatti and G. Busca. J. Catal. 116 (1989) 586.
[35] G. C. Bond and S. Flamerz Tahir, Appl. Catal. 71 (1991) 1.
[36] Y. Ho Kim and Ho-In Lee, Bull. Korean Chem. Soc. 20 (1999) 1457.
[37] Y. Nagai, H. Shinjoh and K. Yokota Appl. Catal. B: Env. 39 (2002) 149.
[38] M. Morán-Pineda, S. Castillo, T. López, R. Gómez, Cordero-Borboa and O. Novarol, Appl. Catal. B: Env. 21 (1999) 79.
[39] S.K. Bej, C.A. Bennett and L.T. Thompson, Appl. Catal. A: Gen (2003), in press.
[40] C. Su, J. Li, D. He, Z. Cheng and Q. Zhu, Appl. Catal. A: Gen. 202 (2000) 81.
[41] G. Centi, Appl. Catal. A: Gen. 147 (1996) 267.
[42] I.E. Wachs and B.M. Weckhuysen, Appl. Catal. A: Gen. 157 (1997)67.
[43] M.A. Reiche, M. Maciejewski and A. Baiker, Catal. Today 56 (2000) 347.